TN 321

Theoretical Notes
Note 321

LA-7386-MS
Informal Report
UC-34
Issued: July 1978

The Time Dependence of the Compton Current and Energy Deposition from Scattered Gamma Rays

J. S. Malik
E. D. Cashwell
R. G. Schrandt

THE TIME DEPENDENCE OF THE COMPTON CURRENT AND ENERGY DEPOSITION FROM SCATTERED GAMMA RAYS

by

J. S. Malik, E. D. Cashwell, and R. G. Schrandt

ABSTRACT

The time dependence of the energy deposition and radial Compton current produced by scattered gamma rays must be known to make better use of the geomagnetic component of the radioflash signal of a nuclear explosion for diagnostic evaluation of the source. To provide a data base for empirical analytic fits to describe this dependence, a series of Monte Carlo calculations of monoenergetic gamma-ray sources in a homogeneous, isotropic air medium were performed and the results fitted with relatively simple and readily usable relations. The results are summarized by graphs and formulae.

I. INTRODUCTION

Gamma radiation is the main generator of radio-frequency signals (radioflash/EMP) resulting from a nuclear explosion. Of the various mechanisms for production of the radioflash fields, the pulse resulting from the deflection of the Compton electrons produced by gamma-ray interactions with the surrounding medium by the Earth's geomagnetic field (GMP) is the dominant mechanism for the high rate of change of the signal amplitude. The time dependence of the GMP is dependent not only upon the time dependence of the gamma-ray source but also upon the modification due to gamma-ray scattering and from the straggling of the Compton electrons behind the gamma rays which produce them. The radiated GMP is from a narrow region of space at ranges up to about eight gamma-ray relaxation lengths (mean free paths of the unscattered radiation) from the explosions. At such distances gamma-ray scattering can markedly broaden the resultant Compton electron current and the electron density, which controls the conductivity of the medium. In most predictions of the GMP they are taken to have the same time dependence--generally that of the source. However, because of the different time-dependent effects due to the scattered radiation, the Compton current and conductivity actually have different time dependences. Despite the large effort expended by Defense Nuclear Agency (DNA) and United States Air Force (USAF) studies on the mechanisms (for high-altitude detonations), the most applicable studies were those of Leipunskii[1] and LeLevier.[2] These, however, do not fully cover the necessary range of distance, time, or gamma-ray energies.

II. MONTE CARLO CALCULATIONS

To extend the data base in gamma-ray energies, time, and radial distance, some monoenergetic Monte Carlo gamma-ray propagation calculations were made to provide the data base for analytic fits as functions of gamma-ray energy, radius, and time of the scattered gamma radiation effects. The calculations used the Monte Carlo code MCNP developed and maintained at the Los Alamos Scientific Laboratory (LASL) by Group TD-6. This general-purpose Monte Carlo code, with three-dimensional geometry and a number of variance-reduction techniques supplied as standard equipment, transports both neutrons and photons[3] (either neutrons alone, photons alone, or the photons produced by neutrons as well as the neutrons) in the same package. Each problem considered a point source of monoenergetic gamma rays in a homogeneous isotropic medium of air with detector weighting functions to predict the energy absorption and radial Compton current in spherical shells about the source. Logging of the two quantities were in terms of retarded time $\tau = t - r/c$. Input parameters to the problems were:

Gamma-ray source energies	:	1, 1.5, 2, 3, 4, 6 MeV
Radii	:	(4, 8, 12, 16) x 10^4 cm
Cutoff radius	:	2 x 10^5 cm
Air density	:	1.1 x 10^{-3} g/cm^3
Energy cutoff	:	0.05 of source energy
Time bin spacing	:	logarithmic, 10 bins/decade
Time cutoff	:	6.33 μs

For what were considered reasonable statistics, the 2, 3, 4, and 6 MeV sources required 5 min of CDC-7600 time; the 1- and 1.5-MeV sources were run for 10 min. The statistics at early times (due to the small time step) and at large range tended to be poor, particularly for the lower energies. This is to be expected as at low energies the angles of scattering are larger and the time delay of the scattered radiation is larger; also, as the transport lengths are shorter there is greater attenuation. As the results were to be fit by an analytic expression, the Monte Carlo results were intended as a guide to the fit expressions; the early-time poor statistics were not of paramount importance as the first time step (1 ns) was about eight times greater than the second, hence the first time bin could be weighted rather highly in the fitting process.

III. ANALYTIC FIT TO MONTE CARLO CALCULATIONS

Empirical fits to the Monte Carlo results for both radial Compton current and energy deposition weighting were made such that the radial Compton current and conductivity could be obtained by a simple fold in the form

$$\sigma(\tau,r,E_\gamma) = \sigma_0(\tau,r,E_\gamma) + B_W(r,E_\gamma) \int_{-\infty}^{\tau} \sigma_0(\lambda,r,E_\gamma)u(\tau-\lambda,r,E_\gamma)d\lambda \quad \text{, and}$$

$$J(\tau,r,E_\gamma) = J_0(\tau,r,E_\gamma) + B_J(r,E_\gamma) \int_{-\infty}^{\tau} J_0(\lambda,r,E_\gamma)v(\tau-\lambda,r,E_\gamma)d\lambda \quad ,$$

where the buildup factors B_J and B_W are time-integrated factors due to scattering and contain the dependence upon distance r. The time-dependent factors u and v are normalized to unity and are only weakly dependent upon distance. Satisfactory fits for both u and v are of the form

$$u,v = Ae^{-St^n} \quad .$$

Normalizing gives

$$A = nS^{1/n} / \Gamma(\tfrac{1}{n}) \quad .$$

$\Gamma(x)$ is the standard gamma function. The fits used for the buildup factors are of the form

$$B = B_1 X^k ,$$

where $X = \mu_t r$ is the number of mean free paths for the unscattered flux. For each gamma-ray energy group there are only two adjustable parameters in each of the factors.

The fits for energy deposition W and for radial Compton current factors are:

$$W = \mu_a E e^{-X} B_W A_W e^{-S_W t^{N_W}} , \text{ and}$$

$$J = \mu_c R_e e^{-X} B_J A_J e^{-S_J t^{N_J}} ,$$

where

$$X = \mu_t \rho r \quad .$$

$$\mu_t, \mu_c, \mu_a$$

are the mass absorption coefficients for transport, Compton scattering of the electron, and energy absorption. The unit is cm^2/g.

ρ = air density in g/cm^3,
r = radius in cm ,
E = initial gamma-ray energy, MeV ,
R_e = mean forward range of the Compton electron in g/cm^2 , and
t = time in units of 10^{-8} s.

The values of the fit parameters are

$$\mu_a E = 0.0283 E^{0.703} ,$$

$$\mu_c R_e = 0.00656 E/(1.0 + 0.0013\ E^3) ,$$

$$\mu_t = 0.0635 E^{-0.52} ,$$

$$S_W = 2.0\ E^{0.2}\ X^{-0.73} ,$$

$$S_J = 2.6\ X^{-0.85} ,$$

$$N_W = 0.5 - 0.3\ e^{-0.36X} ,$$

$$N_J = 0.6 - 0.3\ e^{-0.3X} ,$$

$$B_W = 0.80\ E^{-0.37}\ X ,$$

$$B_J = 0.40\ E^{-0.033}\ X^{1.25E^{-0.15}} , \text{ and}$$

$$A_{W,J} = \frac{N_{W,J}\ S_{W,J}^{1/N_{W,J}}}{\Gamma\left(\frac{1}{N_{W,J}}\right)} .$$

IV. RESULTS

The results of the Monte Carlo calculations and the fitting are summarized in Figs. 1-8.

Figure:

1 Energy buildup factors vs relaxation lengths.

2 Radial Compton current buildup factor vs relaxation lengths.

3 Energy deposition (W) and radial Compton current (J) vs time for 1-MeV source.

4 Energy deposition (W) and radial Compton current (J) vs time for 1.5-MeV source.

5 Energy deposition (W) and radial Compton current (J) vs time for 2-MeV source.

6 Energy deposition (W) and radial Compton current (J) vs time for 3-MeV source.

7 Energy deposition (W) and radial Compton current (J) vs time for 4-MeV source.

8 Energy deposition (W) and radial Compton current (J) vs time for 6-MeV source.

In Figs. 3-8, W is the energy deposition rate in a spherical surface in units of 10^8 MeV cm^2/gs, and J is the electron rate crossing the surface vs time in units of 10^8 electrons/s per source gamma quantum. The unit of time is 10^{-8} s. The surfaces are:

Surface	Radius
1	4×10^4 cm
2	8×10^4 cm
3	12×10^4 cm
4	16×10^4 cm

The air density was 1.1×10^{-3} g/cm^3.

V. CONCLUSIONS

The time and distance dependences of the buildup factors for energy absorption and Compton current are indeed different. The time-integrated energy buildup factors appear to be lower than published dose buildup factors. (Those factors are, however, given for water, which has a higher electron density than air.) While the fits given here could be improved somewhat, they are probably better than is necessary for evaluations using the GMP. It is likely that a linear distance relation and a time dependence proportional to $\exp(-St^{1/2})$ is sufficient and more economic in computer time (that dependence works well to describe the contribution from single-scattered quanta).

ACKNOWLEDGEMENTS

The computer-generated plots were programmed by Judy Coleman.

REFERENCES

1. O. I. Leipunskii, B. V. Novozhilov, V. N. Sakharov, The Propagation of Gamma Quanta in Matter (Pergamon Press Ltd., Oxford, 1965), App. VI.

2. R. E. LeLevier, "The Compton Current and Energy Deposition Rate from Gamma Quanta--A Monte Carlo Calculation," RAND Corporation report RM-4151-PR (June 1964).

3. E. D. Cashwell, J. R. Neergaard, C. J. Everett, R. G. Schrandt, W. M. Taylor, and G. D. Turner, "Monte Carlo Photon Codes: MCG and MCP," Los Alamos Scientific Laboratory report LA-5157-MS (March 1973).

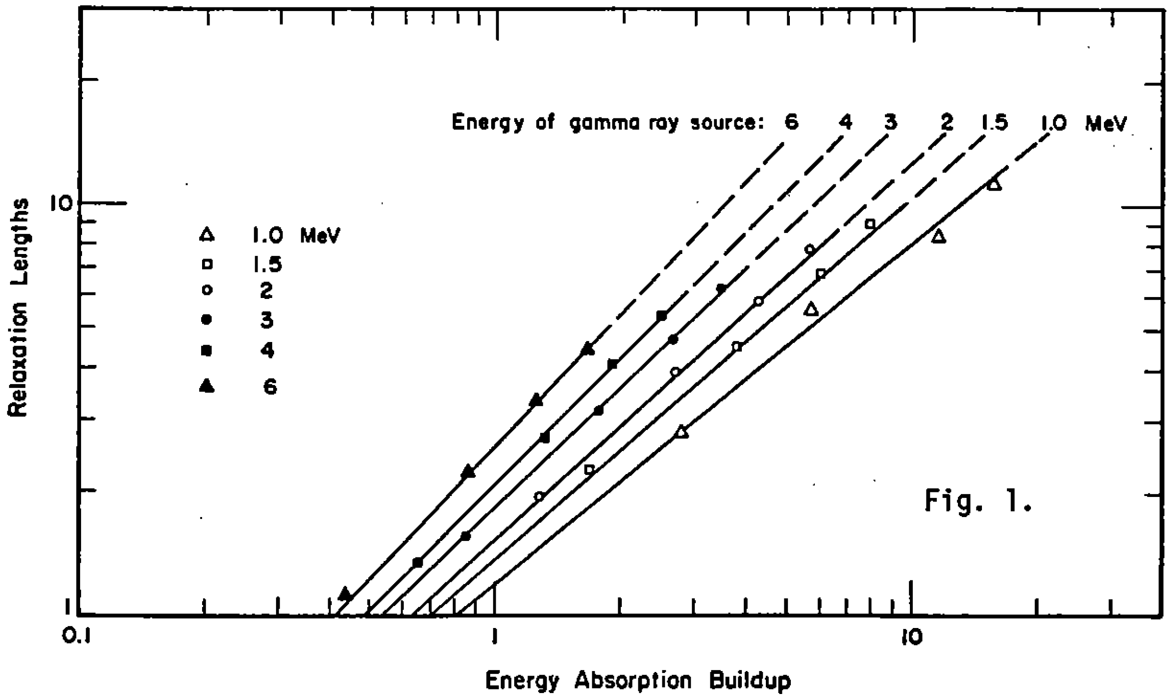
Energy of gamma ray source: 6 4 3 2 1.5 1.0 MeV
1.0 MeV
1.5
2
3
4
6
Relaxation Lengths
10
1
0.1
1
10
Energy Absorption Buildup

Fig. 1.

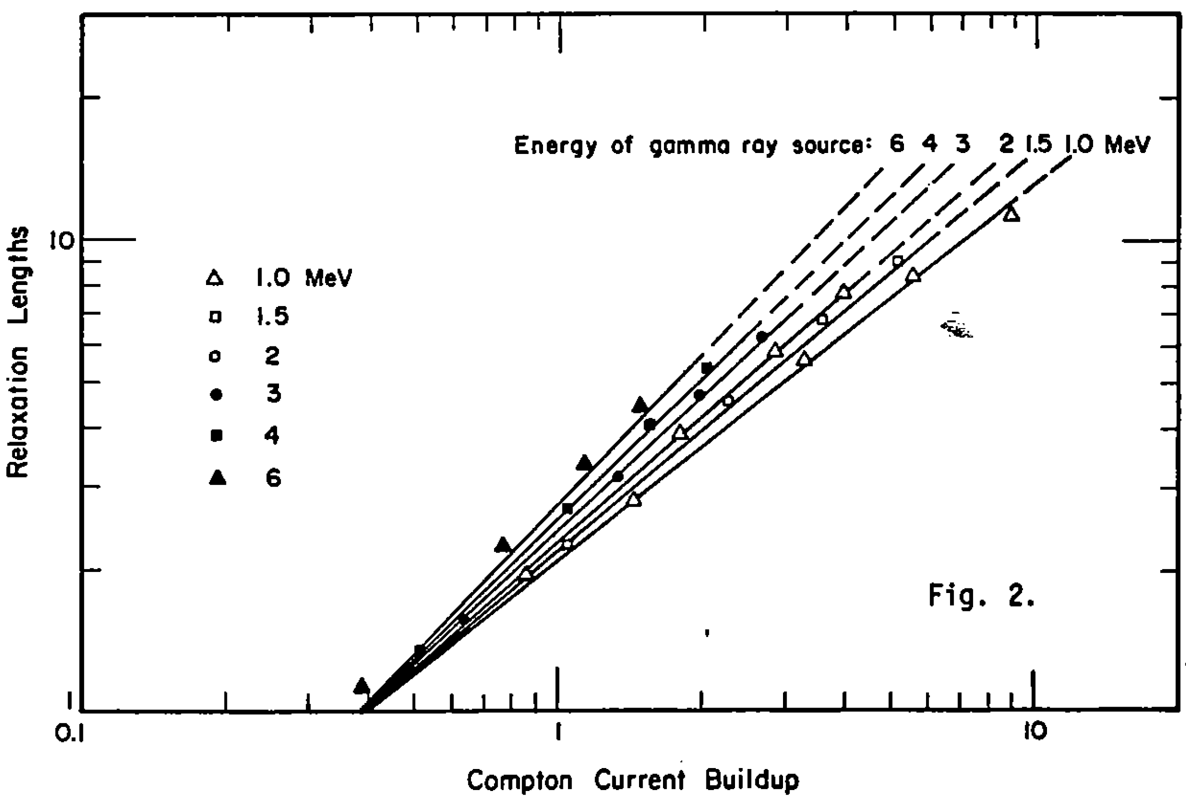
Energy of gamma ray source: 6 4 3 2 1.5 1.0 MeV
1.0 MeV
1.5
2
3
4
6
Relaxation Lengths
10
1
0.1
1
10
Compton Current Buildup

Fig. 2.

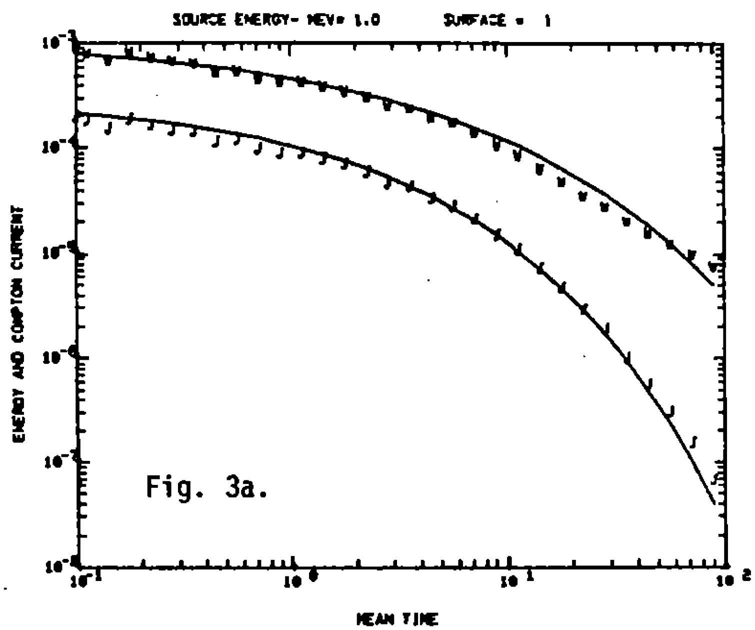

Fig. 3a.

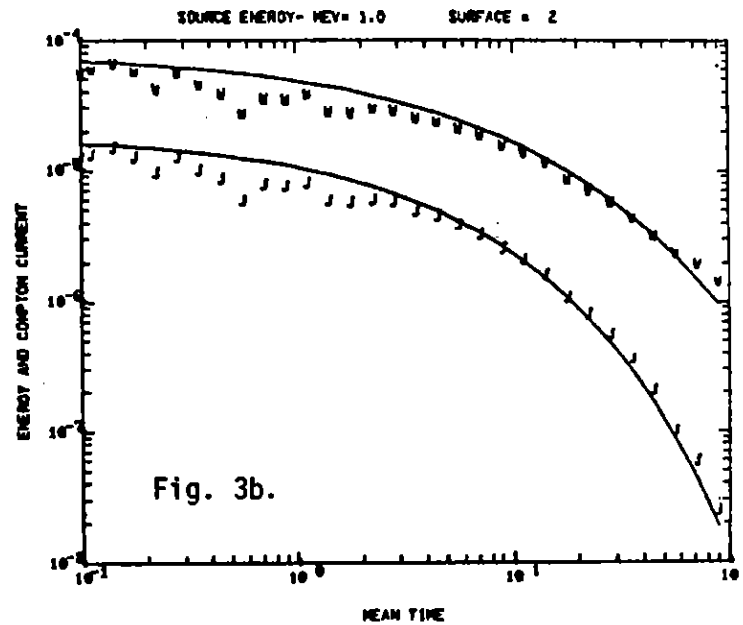

Fig. 3b.

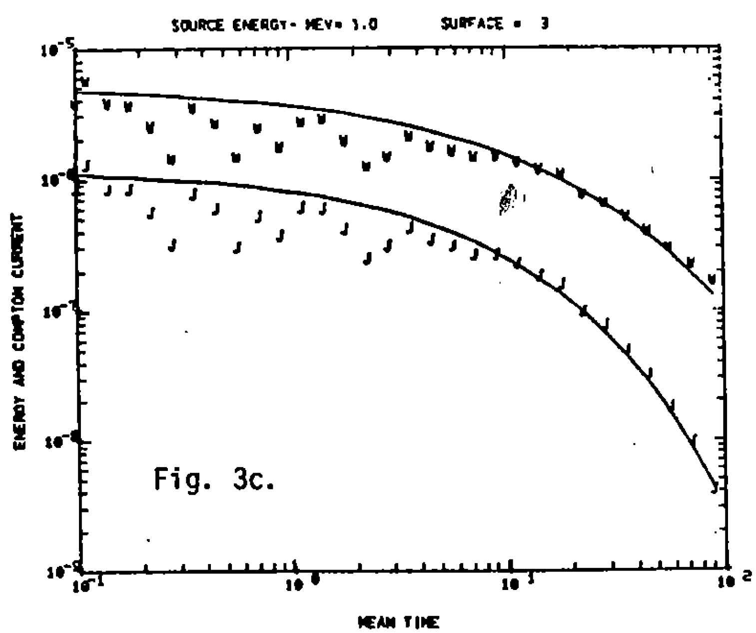

Fig. 3c.

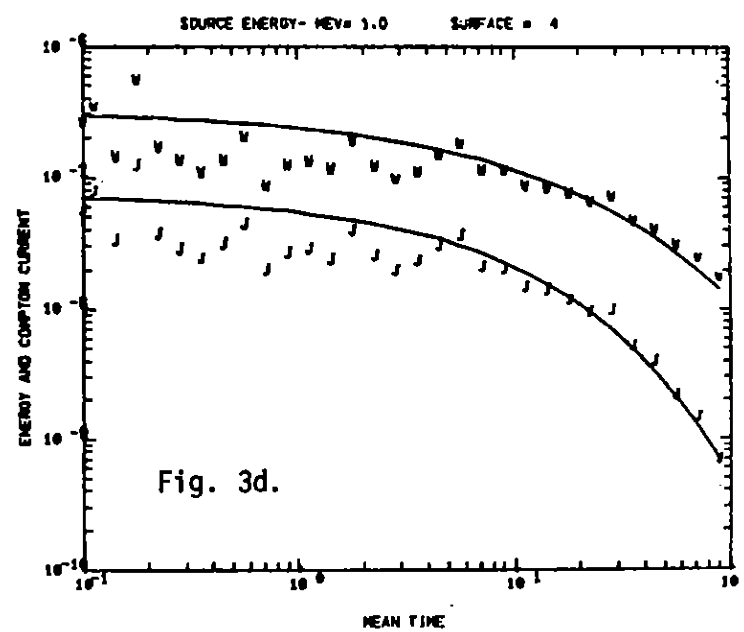

Fig. 3d.

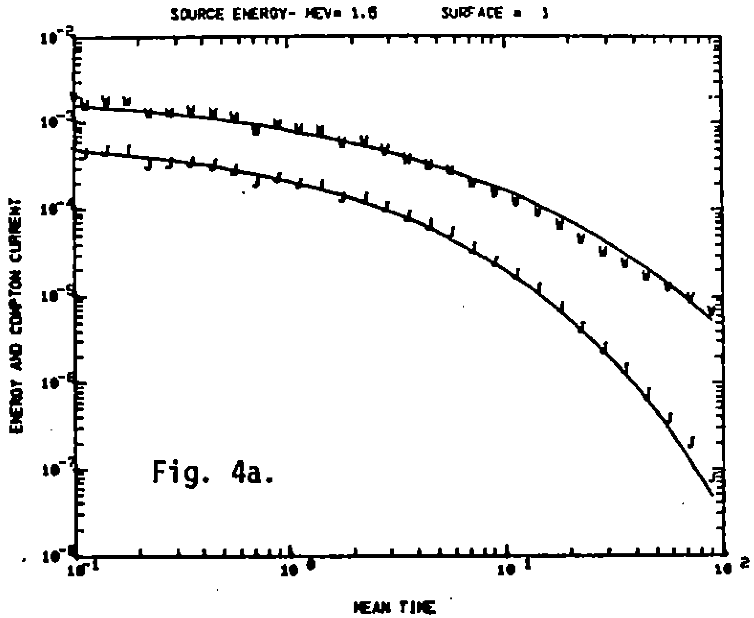

Fig. 4a.

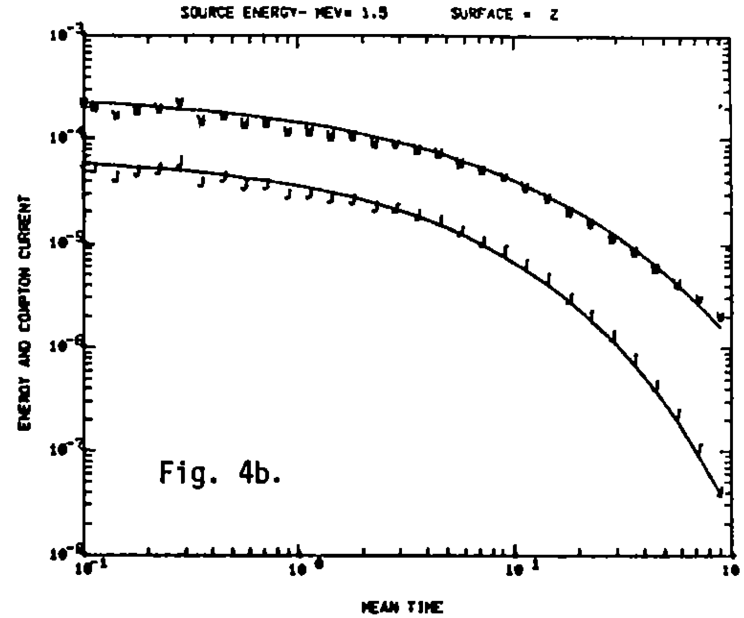

Fig. 4b.

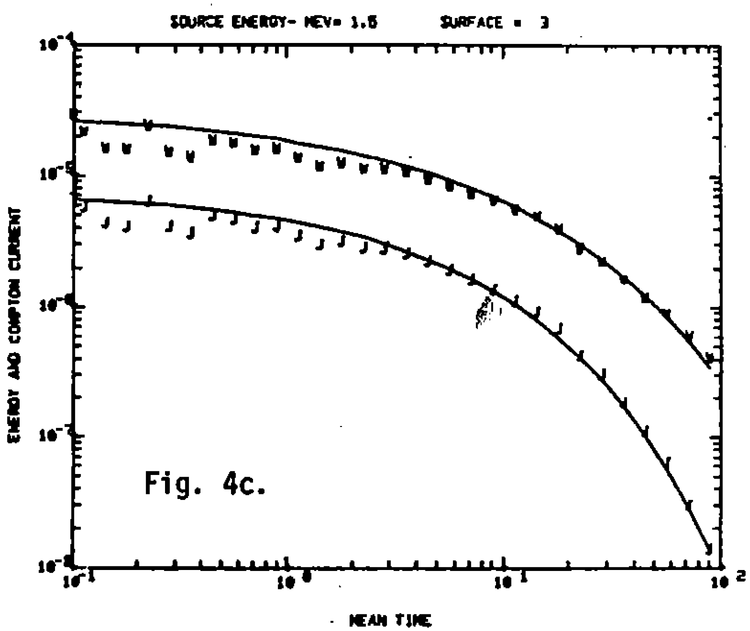

Fig. 4c.

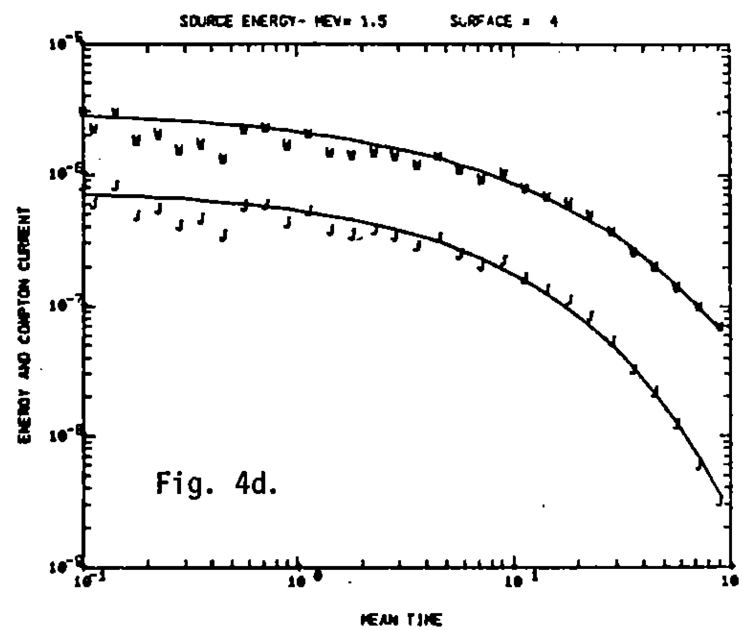

Fig. 4d.

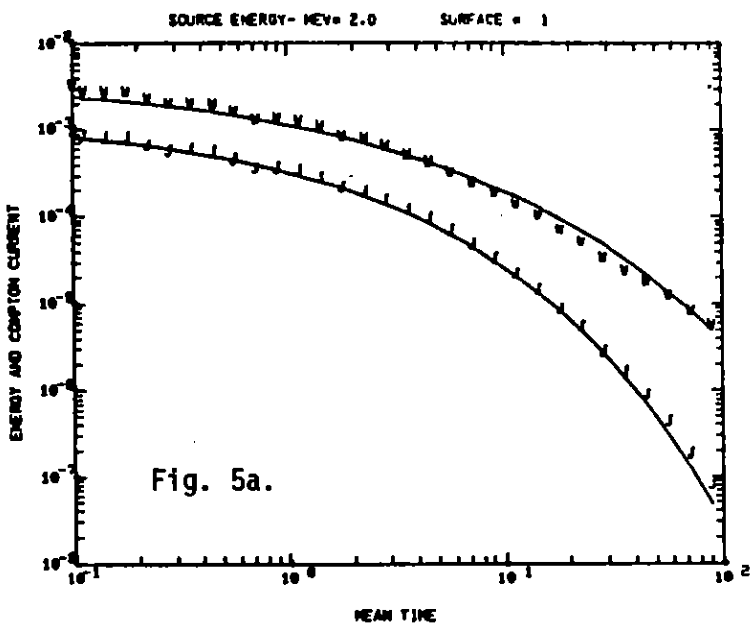

Fig. 5a.

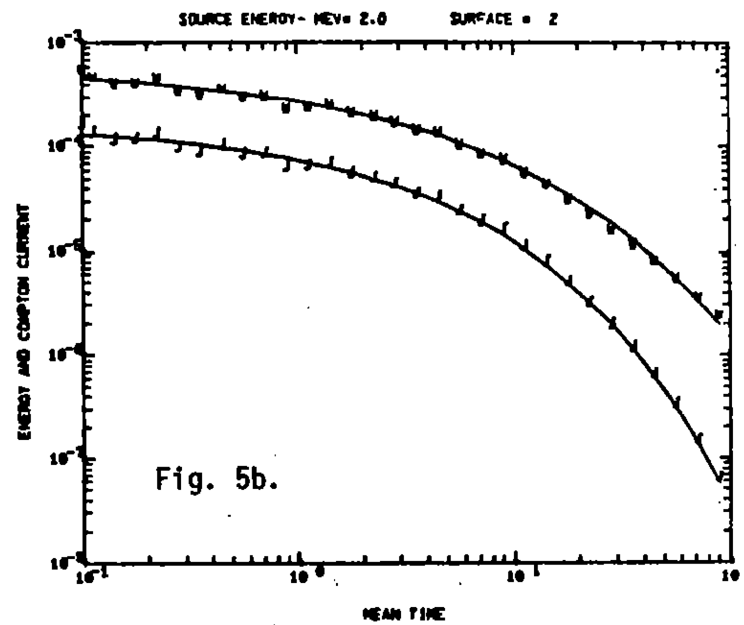

Fig. 5b.

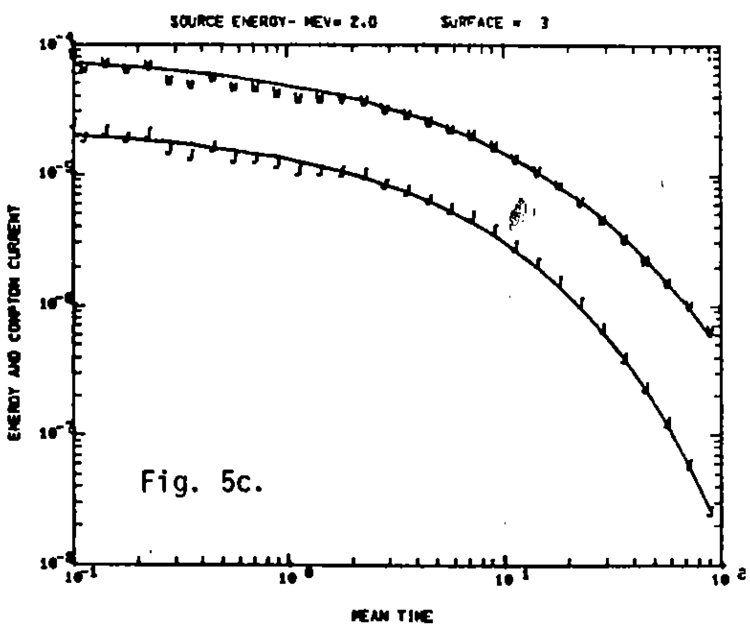

Fig. 5c.

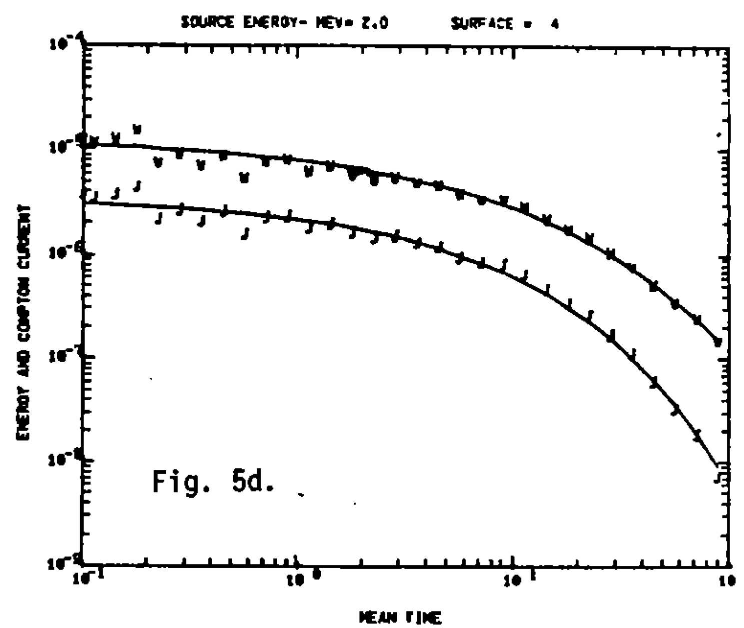

Fig. 5d.

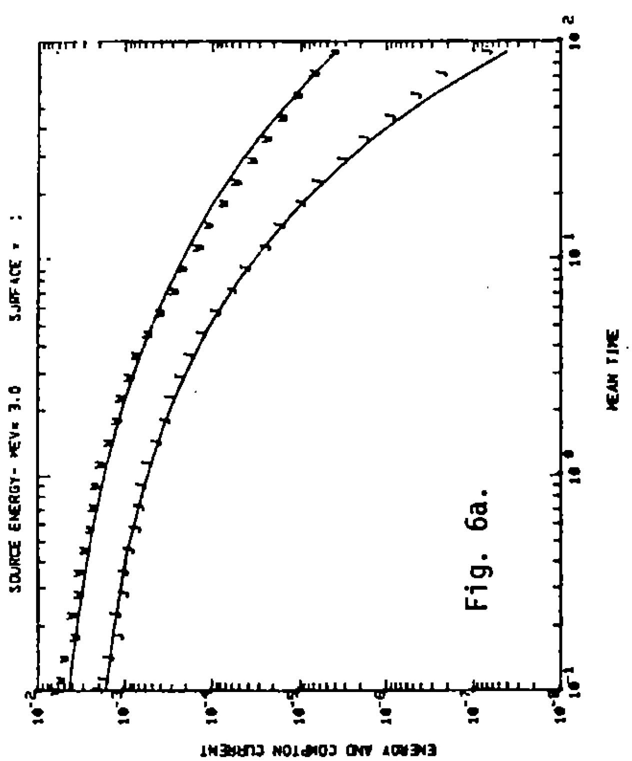

Fig. 6a.

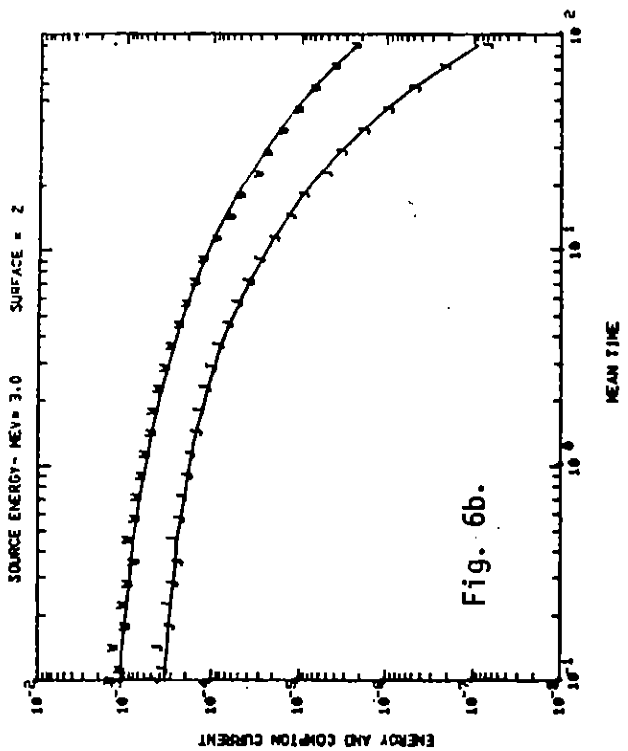

Fig. 6b.

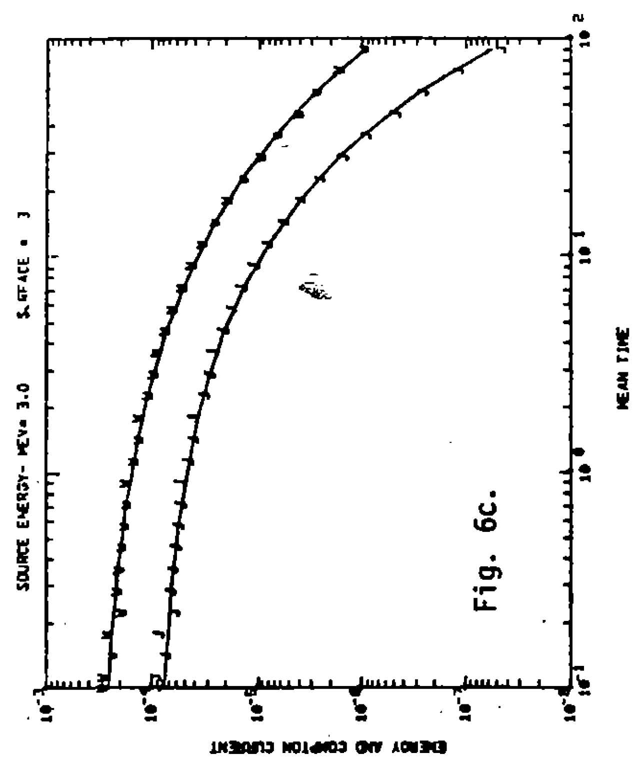

Fig. 6c.

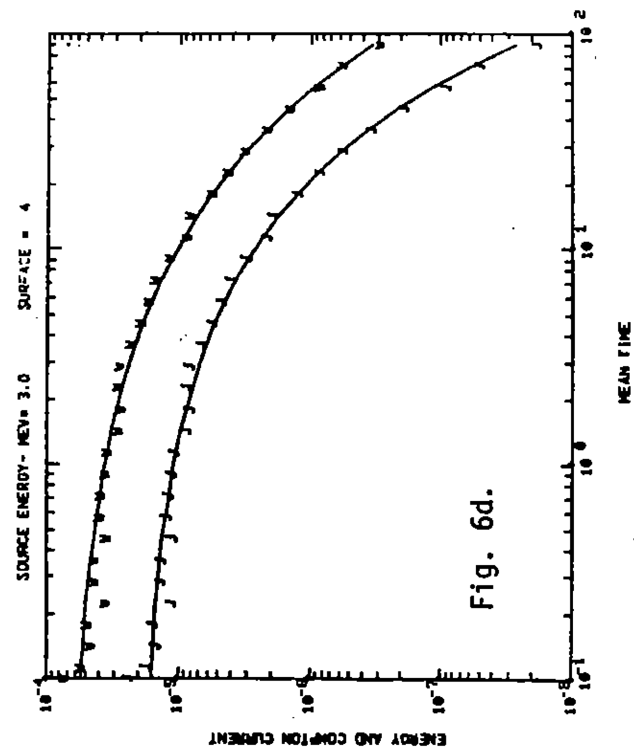

Fig. 6d.

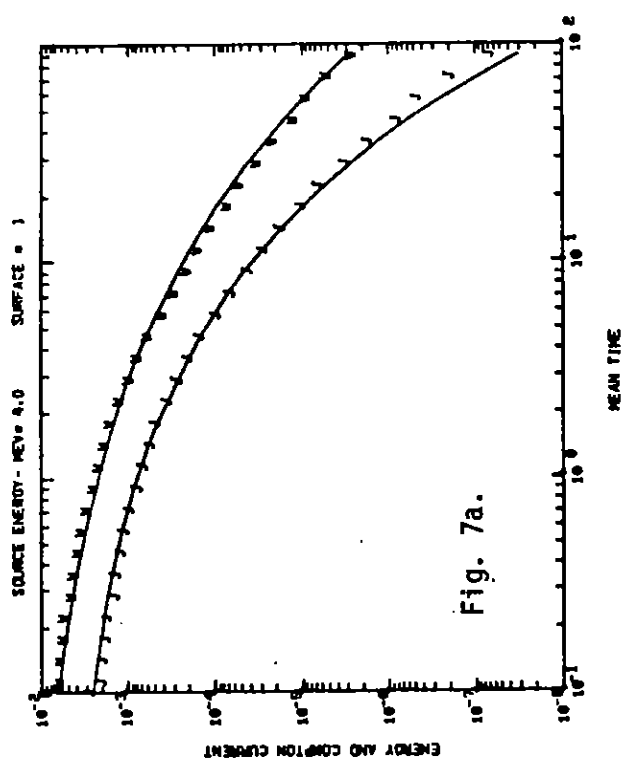

Fig. 7a.

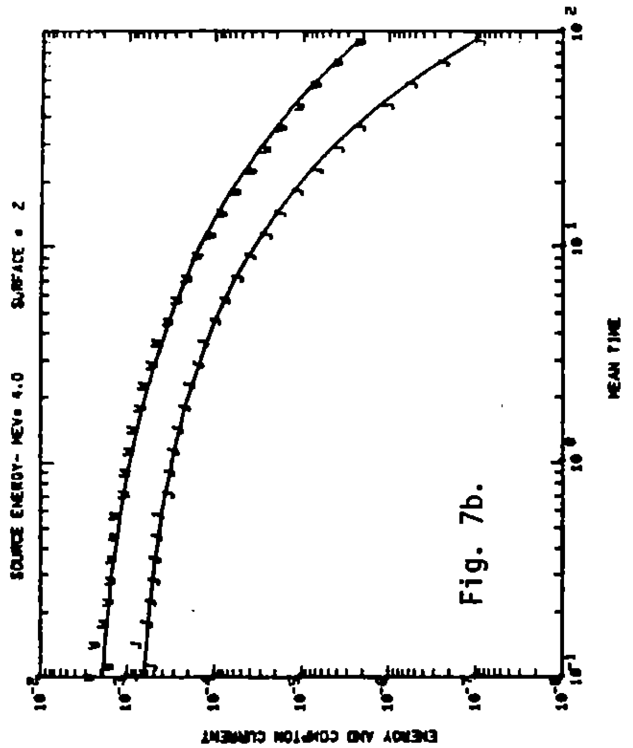

Fig. 7b.

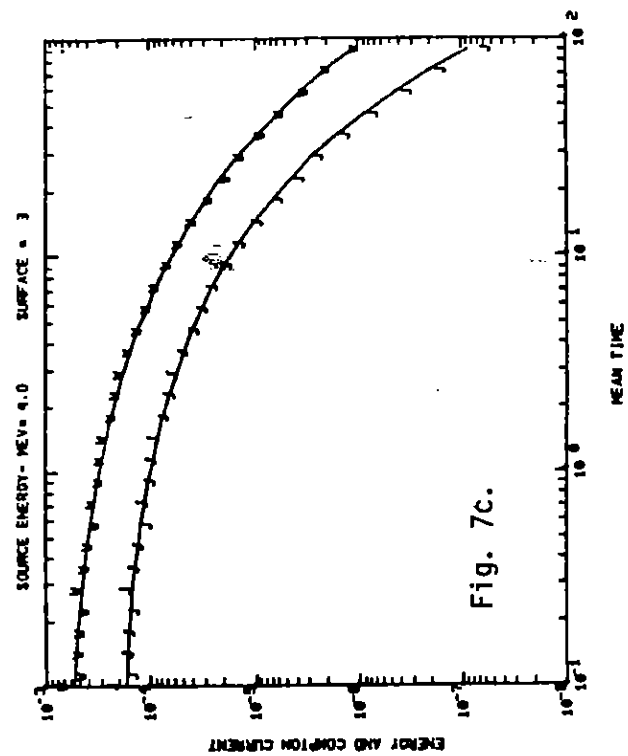

Fig. 7c.

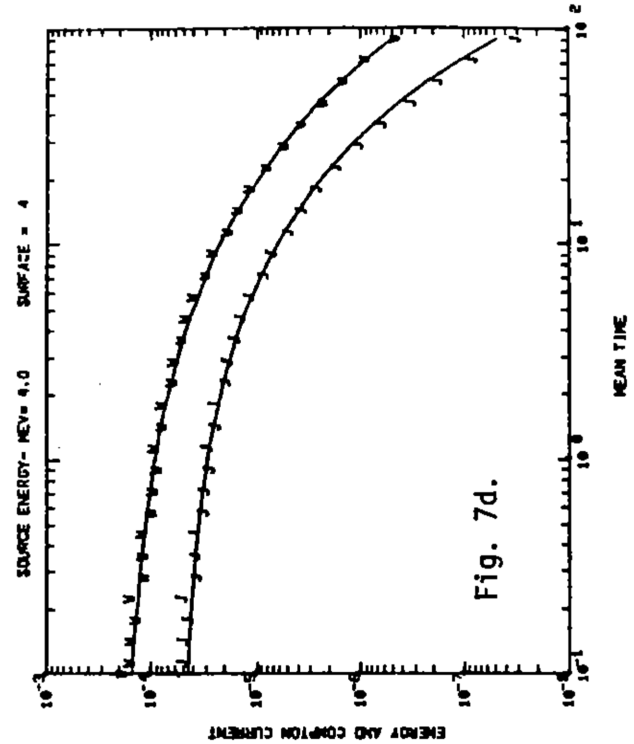

Fig. 7d.

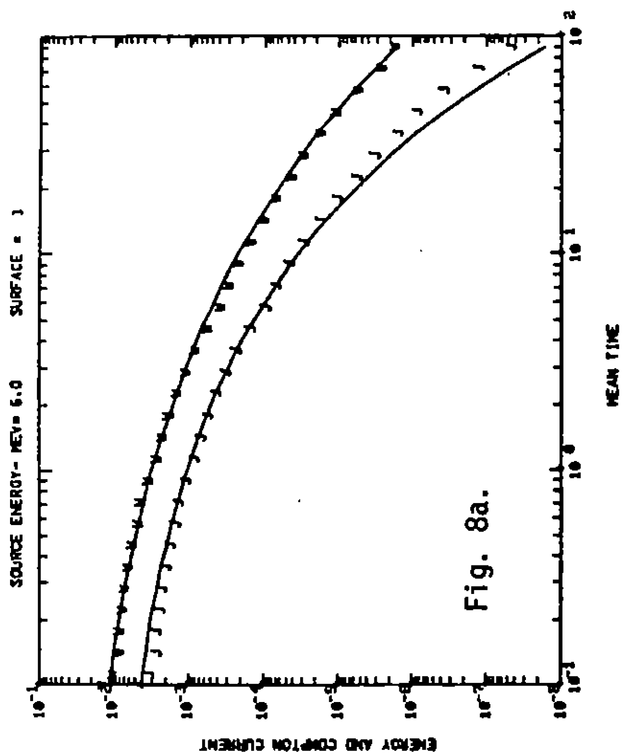

Fig. 8a.

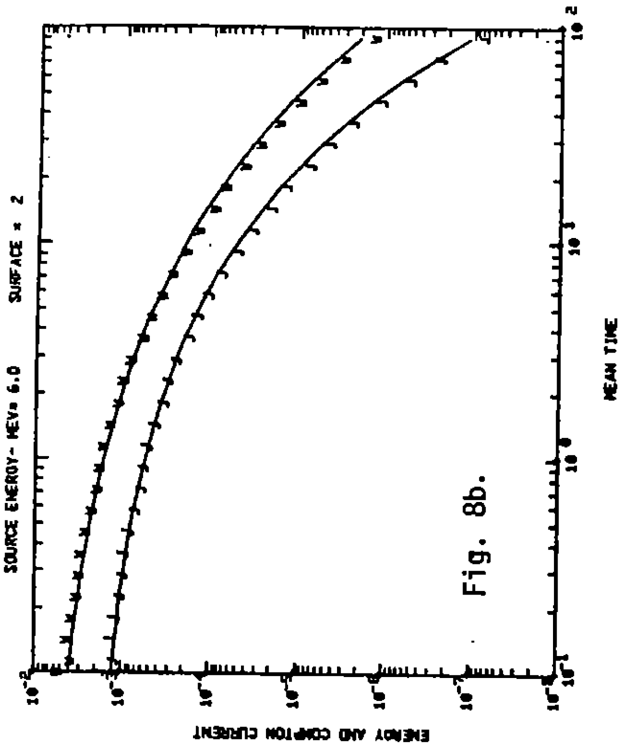

Fig. 8b.

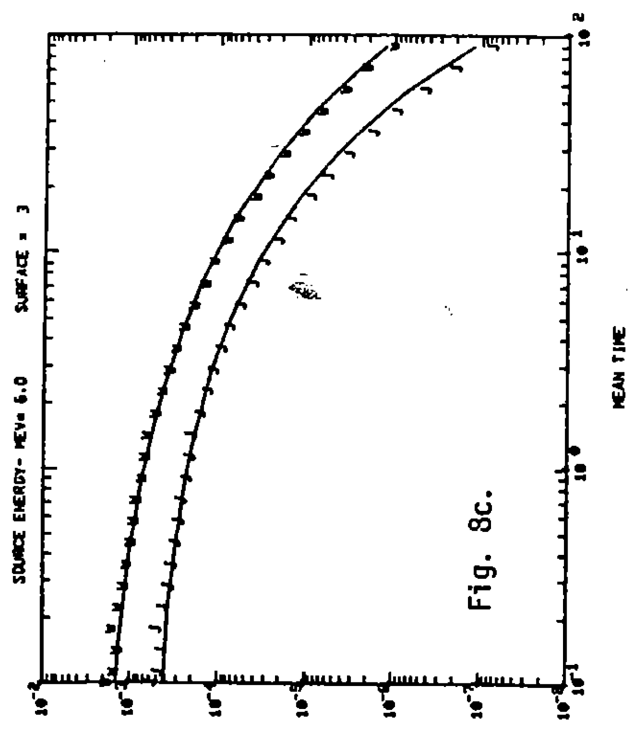

Fig. 8c.

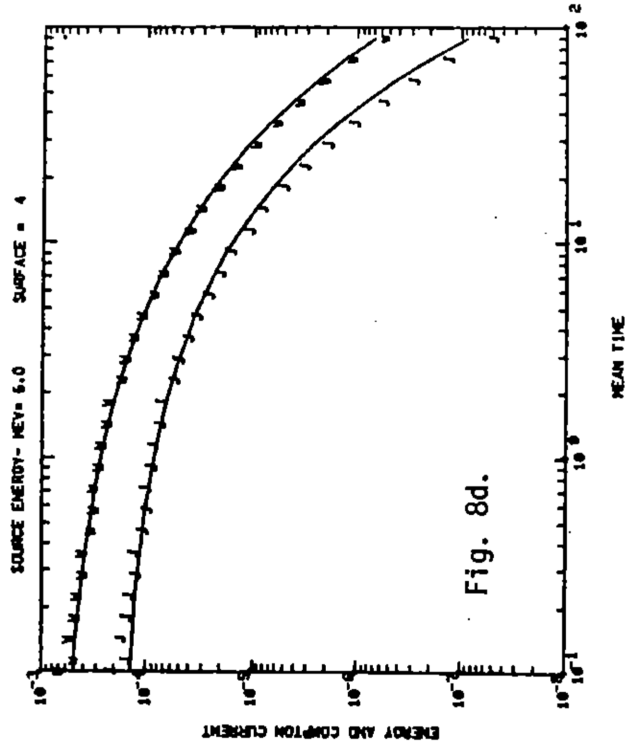

Fig. 8d.